SMGroup

SM Journal of Forensic Research and Criminology

Research Article

Chemically Modified Piezoelectric Devices to Detect Seized Marijuana and Cocaine Samples: A New Tool for Forensic Chemistry

Matheus MMT de Menezes[1,2], Marco A Balbino[1], Alex S Castro[1], Izabel C Eleotério[1], Grégoire Jean-François Demets[1], Osmair V de Oliveira[2], Antonio J Ipólito[3], Bruce R McCord[4] and Marcelo F de Oliveira[1]*

[1]*Departamento de Química, Grupo de Estudos em Eletroquímica e Química Forense, Faculdade de Filosofia, Ciências e Letras de Ribeirão Preto, Brazil*

[2]*Instituto Federal de Educação, Ciência e Tecnologia de São Paulo, Brazil*

[3]*Núcleo de Perícias Criminalísticas de Ribeirão Preto, Superintendência de Polícia Técnico-Científica do Estado de São Paulo, Brazil*

[4]*Department of Chemistry, Florida International University, United States*

Article Information

Received date: Feb 28, 2017

Accepted date: Apr 28, 2017

Published date: May 04, 2017

***Corresponding author**

Marcelo Firmino de Oliveira, Departamento de Química, Grupo de Estudos em Eletroquímica e Química Forense, Faculdade de Filosofia, Ciências e Letras de Ribeirão Preto, USP, 14040-901, Ribeirão Preto, Brazil;

Tel: 55-16-3315-9150;

Fax: 55-16-3315-9101;

Email: marcelex@usp.br

Keywords Forensic chemistry; Cannabinoids; cocaine; quartz crystal microbalance; chemical modifiers

Abstract

Cannabinoid gas-phase detectors were assembled modifying piezoelectric quartz crystals with Fast Blue B salt, Triton X-100, and Nafion-coated Fast Blue B salt. A similar sensor was assembled using cucurbit (6) nuril for modifier to detect cocaine in the gas-phase. Several analyses were carried out with seized drug samples, and the amount of cannabinoids or cocaine adsorbed on the sensors was calculated using Sauerbrey equation. Moreover, PM7 semi empirical calculations were used to understand the adsorption processes in these systems. Fast Blue B salt coated with a thin Nafion layer for cannabinoids and cucurbit (6) uril for cocaine provided stable and reversible responses during the analyses of several seized samples. Theoretical calculations support their affinity towards the analytes, and our results show that it is possible to assemble reliable piezoelectric sensors for cannabinoids and cocaine.

Introduction

Cannabis and cocaine (COC) are widely used illicit drugs are illicit drugs [1]. The primary psychoactive substance of Marijuana is named Δ^9-tetrahydrocannabinol (Δ^9-THC; 6a, 10a-trans-6a,7,8,10a-tetrahydro-6,6,9-trimethyl- 3-pentyl-6H-dibenzo [b,d] pyran-1-ol) and its use was associated of development of psychosis [2,3]. COC ($C_{17}H_{21}NO_4$ or methyl (1R, 2R, 3S, 5S)-3-(benzoyloxy)-8-methyl-8-azabicyclo [3,2,1] octane-2-carboxylate) is an alkaloid extracted from Erythroxylum coca. It stimulates the central nervous system and its abuse may cause several adverse effects as anxiety, organ damage, and cardiac arrest. When injected, it helps spreading of human immunodeficiency syndrome [4-9]. When these drugs are apprehended, they are detected and identified by several (and expensive) techniques. An analysis protocol should be followed as recommend by the United Nations (UN) and the Drug Enforcement Administration (DEA) Scientific Working Group for the Analysis of Seized Drugs (SWGDRUG) [1,9,10]. Colorimetric test for Cannabis is carried out with Fast Blue B salt (FBB) or Duquenois–Levine (D-L) reagents after the extraction of cannabinoids in organic media. Color changes (purple-red for FBB or blue for D-L) indicate the presence of Δ^9-THC and other cannabinoids (Cannabinol, CBN; cannabidiol, CBD) [10]. Scott test, with a solution of cobalt thiocyanate, is indicated for seized COC samples. Positive tests reveal a bluish color which turns to pink after the addition of hydrochloric acid and it should turn blue again with the addition of chloroform. [9,11]. Colorimetric tests, however, are subjected to false positive or false negative tests [11,12].

Nowadays, there is a strong interest in developing novel and cheap methods to analyze illicit drugs. Quartz Crystal Microbalance (QCM) measures the shift of resonance frequency of a piezoelectric quartz crystal during mass changes by adsorption/desorption processes [13-17].

Piezoelectricity is basically the generation of an electric field upon mechanical pressure which depends on the molecular asymmetry [18-21]. Materials such as AT-cut type transverse mode alpha quartz crystals, lack symmetry center, and display such effect [13-15]. A single crystal of this quartz will vibrate under oscillating electric fields, and its resonance frequency is dependent of its mass.

Any variation in crystal's mass, by adsorption of some molecule for example, shifts its resonance frequency. Such frequency shifts are associated with mass by the Sauerbrey equation (eq. 1) [18,19,20].

$$\Delta F = \frac{-2.3x10^6 F_0^2 \Delta M}{A} \quad \text{Eq. 1}$$

OPEN ACCESS

ISSN: 2574-2426

Where ΔF is the frequency shift (Hz), F is the original resonance frequency before coating (MHz), ΔM is the mass variation (g), and A is the exposed crystal area (cm^2).

Piezoelectric micro-gravimetry extremely sensitive to mass variations with estimated detection limits around 10^{-12} g [21].

Piezoelectric sensors find many applications in several fields, including humidity sensors [22-27], thermometers [28], detection of aerosols and suspended particulates [29-33], measurement of evaporated metal films thickness [34,35], adsorption phenomena [36,37], barometry [38,39], and speed and corrosion investigations [40]. These sensors were also useful to detect gaseous pollutants [41,42], to determine hydrocarbons and polar compounds in water [22,43-45].

This device can offer come advantages when a surface of the QCM is chemically modified with a substance. Increased selectivity and sensitivity towards a specific analyte may be achieved by chemically modifying the QCM sensor surface [46-49]. Some authors have proposed different piezoelectric sensors to analyze COC [50-54] and other illegal drugs [46] over the last years. Hunt et al. [50], for example, modified metal electrodes coupled to quartz crystals with benzoylecgonine antibody to detect COC in the vapor phase at ng L^{-1} levels. Other papers consider the affinity of COC toward cholinesterase inhibitors to build piezoelectric sensors [52], or report the detection of COC using the immunosensors-coated CQM [53]. A label-free, real-time piezoelectric aptasensor COC was assembled using an Electromagnetic Piezoelectric Acoustic Sensor (EMPAS) [54].

Several reagents could be used as QCM modifiers for such purpose, and many of them are already used for reaction with Δ^9-THC and COC in other detection/analysis systems and processes.

FBB reagent (3,3'-dimethoxybiphenyl-4,4'-bisdiazonium chloride, Figure 2), is widely used for screening Cannabis sativa L. in colorimetric tests, and it was used successfully as a derivatizing agent for voltammetric analysis of Δ^9-THC [55]. FBB is widely used for colorimetric test for marijuana samples. The positive test generates a reddish color, indicating that specific interactions between FBB and cannabinoids occur, and justifies its use as chemical modifier.

Triton X100 (TX, Figure 2c) is a non-ionic surfactant as isopolyoxyethylene derivative containing a hydrophobic alkyl phenyl group [56,57]. It is widely used in biology and biochemistry laboratories, precisely because they are agents which act on the surface, thus enabling transport in cells. The applications of the TX as modifier can be attributed to investigate the enhancement effects of surfactants, and the interactions such as adsorption on the surface of the electrode and redox reactions [58]. The literature reports the versatility of Nafion (1,1,2,2-tetrafluoro-2-[1,1,1,2,3,3-hexafluoro-3-(1,2,2-trifluoroethenoxy)propan-2-yl]oxyethanesulfonic acid), a fluoropolymer used as modifiers for determination of several compounds [59-62]. Their application on the surface electrode showed sufficient stability and it can provide better selectivity in electrochemical detection [60-62]. Cucurbit (6) uril (CB[6]), is barrel-shaped cavitand produced by the six glycoluril units and formaldehyde under acidic conditions [63-68]. CB (6) has produced good results when used as a chemical modifier for detecting 4,4-oxydianiline [64], 3,4-methylenedioxymethamphetamine [65], and acetylcholine [66].

In the present paper, we have used 3 different quartz-crystal modifiers (Figure 2) to prepare piezoelectric sensors for the analysis of Δ^9-THC and 1 for COC in the gas phase. We have monitored mass variations during drug-loaded vapor flow over the sensors, to assess strength and reversibility of the interactions between the chemical modifiers and the analytes. In addition, theoretical calculations were realized for a better understanding of the adsorption/chemisorption processes at the chemical modifiers interfaces

Experimental

Our study was conducted in partnership with the laboratory of toxicological analysis Institute of Criminalistics, Ribeirão Preto, São Paulo state, Brazil.

Hexane cannabis extract was stored in a glass tube in a kiln at 30 ºC.

Commercial AT-cut type quartz crystals (fundamental freq = 10 MHz) were mounted on a HC-6/U (Universal Sensors) ceramic support model. All the crystals (diameter of 10-14mm, 0.15 mm thick) had thin gold layer electrodes (diam. 6-8 mm; 3000-10000 Å thick) on both sides.

Chemical coating modifiers

The piezoelectric crystals were carefully modified in a reproducible way because this process can affect the sensitivity, stability, and lifetime of the resulting sensor. FBB, FBB with Nafion, and TX (Figure 1a, 1b, 1c) were used to modify the piezoelectric sensors, which were later employed to analyze Δ^9-THC (Figure 1d) in seized samples. The investigation of detection of COC was performed using CB (6) as chemical modifier.

The chemical modifiers were dissolved in acetonitrile and transferred to the center of the gold electrodes. All the process was performed manually. The piezoelectric crystals were carefully modified in a reproducible way because this process can affect the sensitivity, stability, and lifetime of the resulting sensor.

Generation of drug vapor

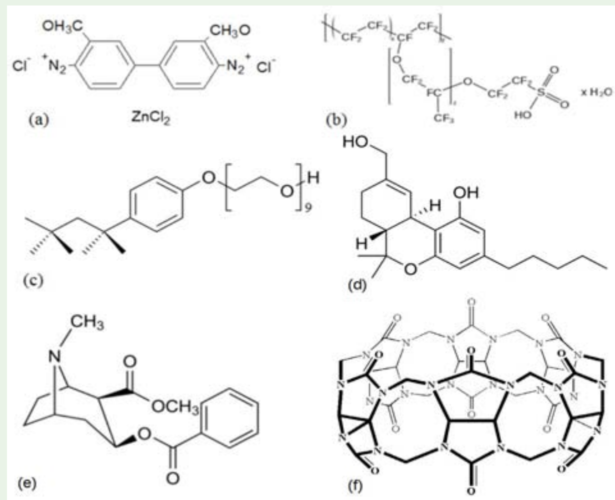

Figure 1: Chemical structures of (a) FBB, (b) Nafion, (c) TX, (d) Δ^9-THC, (e) COC, and (f) CB (6).

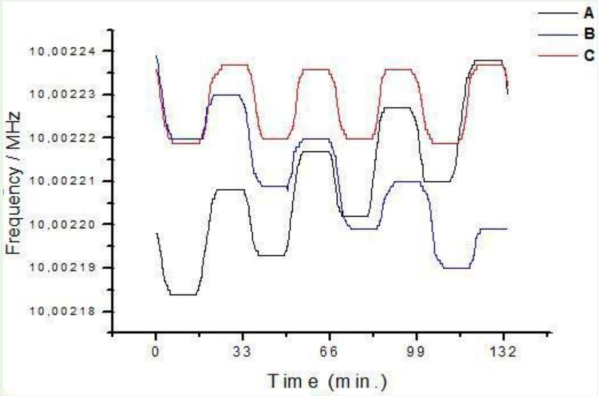

Figure 2: Frequency (MHz) versus time (min) for the cannabis extract using a piezoelectric sensor modified with: a) FBB salt; b) Triton X-100; c) FBB salt and Nafion.

In a furnace at 50 ºC, A constant flow of N_2 (100 $mL.min^{-1}$) passed in a glass tube containing the samples. It has with two opening for gas inlet, and other from where the drug-loaded gas reaches the piezoelectric sensor casing.

The Piezoelectric system

After the piezoelectric crystals were coated with the appropriate chemical modifier, they were placed in a glass cell (with both faces exposed to the drug vapor) and connected to an OT-13 (International Crystal Mfg. Co, Oklahoma City, OK) oscillator to keep them vibrating at constant frequencies. The oscillator was powered with 9 volts DC using a regulable voltage source (Heathkit, Model IP-2728). The output frequency of the oscillator and the crystal was recorded on a FC Goldstar 2015 digital frequency meter.

The physical configuration of the glass cell containing the piezoelectric crystal influences the analytical sensitivity. The gas flow was divided to two equal parts, to reach directly and simultaneously both sides of the chemically modified crystal. This improves significantly the contact between the drug and the piezoelectric sensor.

Each measurement lasted 10 minutes to saturate the analyte/modifier interaction sites and to ensure that frequency would not change. However, within each essay, it remained constant in triplicate experiments.

Theoretical method

Δ^9-THC and COC structures as well as their complexes with the Chemical Modifiers (CM) to say TX, FBB, and CB (6) were optimized using the semi empirical PM7 [69] method implemented in MOPAC2012 package [70]. Although the semi-empirical is less precise than ab initio methods, they provide satisfactory results for large chemical systems as ours, at a low computational. Furthermore, semi empirical methods can provide excellent results for dimeric systems involving Van der Waals interactions as show by Li [71] and Brandenburg [72]. Reactivity parameters were calculated from the HOMO (highest occupied molecular orbital) and LUMO (lowest unoccupied molecular orbital) energies. Binding energies (E_b) between the modified and Δ^9-THC or COC were calculated using the following equation,

$$E_b = E_{ndrug\text{-}CM} - (E_{ndrug} + E_{CM})$$

Where $E_{ndrug\text{-}CM}$ is the total electronic energy of the ndrug-CM complexes, and n=1 or 2n, E_{ndrug} and E_{CM} are the total energy of the drugs and the chemical modified alones, respectively.

Results and Discussion

Piezoelectric sensors for Cannabinoids

Coating: Sensors built with pure FBB or TX as chemical modifiers are not adequate for cannabinoids detection. Despite significant frequency variations during the analyses, the signal baselines are not stable. In the case of FBB, a clear desorption problem arises [73]. Mass is lost during the experiment, and the base frequencies (resonance frequency in the absence of analyte) rise gradually, starting at 10.0022 MHz, and shifted to 10.002235 after 4 gas injections. This indicates clearly that FBB is lost during the analysis, and that the interaction of FBB and gold surface is weak (Figure 2a).

The opposite behavior is verified with pure TX coatings. Base frequencies decrease over time, during successive sample injections. Cannabinoids do not desorb off the modifier indicating that very strong interactions occur between the cannabinoids and TX (Figure 2b). Lifetime and reproducibility of the analyses using the TX-modified transducer was considerably smaller when compared to FBB. It is very difficult to avoid irreversible adsorption over a chemically modified surface, but it is relatively easy to enhance adsorption of a chemical modifier over a metallic surface [73]. For this reason, we have used Nafion to protect the modifying layer, and to reduce FBB mass loss.

The transducer was initially coated with a FBB film which was covered by a Nafion film. The system was fully reversible in at least one of triplicate experiments in the same sequential crystal.

This time, the sensor is stable and frequency variations are constant during successive sample injections (Figure 2c).

Using the best piezoelectric system to analyze cannabis extract – electrode coated with FBB and Nafion, the reaction time that would give an optimal signal without losing reliability was monitored [73].

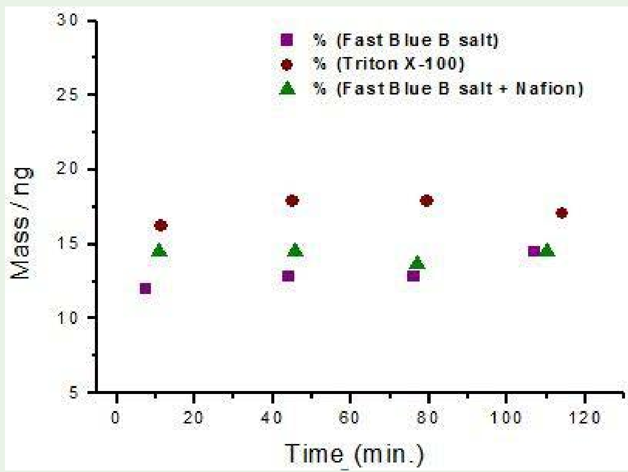

Figure 3: Adsorbed mass of the cannabis extract (ng) versus time (min) for the modified piezoelectric sensors studied here.

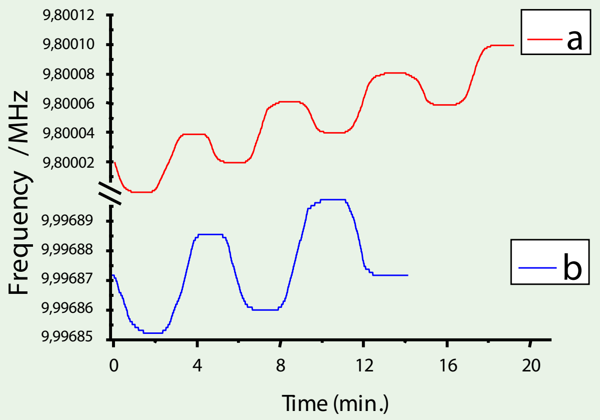

Figure 4: Frequency response versus time (minutes) for COC standard (a) and seized (b) samples by piezoelectric analysis using CB (6) as chemical modifier.

One minute analysis can identify cannabinoids in Cannabis extract. The total mass of adsorbed analyte was measured as a function of time for each modifier (Figure 3).

The TX-modified transducer has adsorbed the larger mass of analyte modified with FBB and a thin layer of Nafion adsorbed larger mass of cannabinoids in the gas phase.

Analysis of COC and its interferents with CB (6) modified transducers

When CB (6) is used as a modifier, a variation of frequency in 20 Hz was observed. This behavior was consistent in a triplicate analysis for COC (standard and seized samples). A lower adsorption of mass indicates a semi-reversible system. Figure 4 shows a response between COC samples and piezoelectric sensor chemically modified with CB (6) (Figure 4):

After each cycle of analysis, the frequency is increased on the saturation level of interaction sites. Figure 8 illustrates the interaction purposed between COC and CB (6) (Figure 5):

CB (6) molecule have an inner and outer diameter and inner cavity greater than CB (5) modifier [67]. CB (5) is a cucurbituril with ten carbonyl groups. Thus, the size of cucurbiturils has an

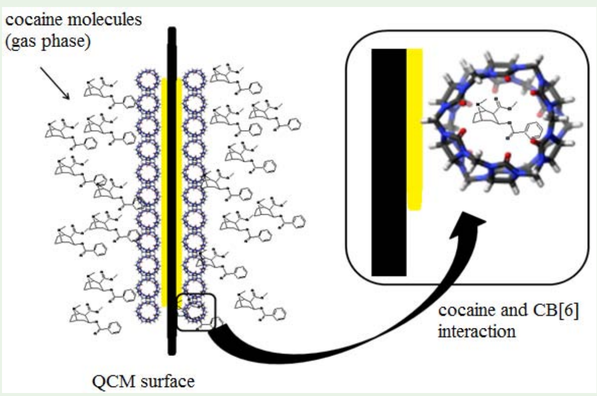

Figure 5: Purposed interaction process between COC standard sample (gas phase) and CB (6) (Illustration unscaled).

Table 1: Results of frequency variation (Hz) obtained for COC (standard and seized sample) and their main interfering substances.

Frequency Variation ΔF / Hz		
Substance	**COC (standard)**	**COC (seized)**
No modifier	0	0
CB (5)	0	0
CB (6)	20	20

influence on the chemical interactions involving the analytes studied [68]. For COC samples (standard and seized), the sensitivity of the piezoelectric sensor using this modifier has shown better results. Using this modifier to detect interfering substances, different results (obtained for COC analysis) were observed. The piezoelectric analysis of interfering substances using CB (6) has shown a frequency variation for caffeine and theobromine between 11 and 12 Hz, respectively. This behavior can be attributed to their similar molecular structure, where a methyl group differentiates these substances. However, these results obtained were different when compared with to COC and lidocaine. This material, commonly added in COC seized samples, did not show a resonant frequency variation.

Table 1 lists the results for COC and interfering substances with/without cucurbiturils as a chemical modifier on the (gold) surface of piezoelectric sensors. The sensitivity of this method is observed when CB (6) is used as the modifier in the piezoelectric sensor. The absence of frequency variations when piezoelectric sensors were not chemically modified shown no physical and chemical interactions between this device and COC with interfering substances studied.

Semi empirical calculations

Semi empirical calculations using the PM7 Hamiltonian were realized to understand the adsorption processes on the piezoelectric transducers at the atomic level. From lowest energy conformations, we could picture stable molecular assemblies (Figure 6) this way.

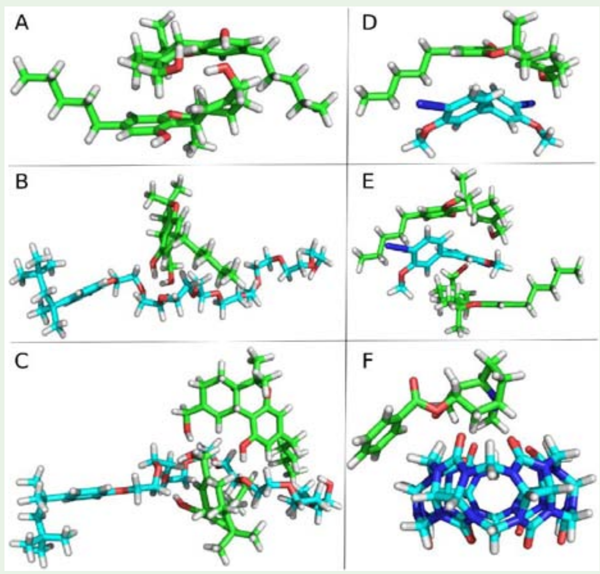

Figure 6: Optimized structures of the complexes obtained at Hamiltonian PM7 method. A) Δ^9-THC-Δ^9-THC, B) Δ^9-THC-FBB, C) $2\Delta^9$-THC-FBB, D) Δ^9-THC-TX, E) $2\Delta^9$-THC-TX, and F) COC-CB [6]. Hydrogen in white, carbon in green, nitrogen in blue, oxygen in red, and cyan colors for drug abuse and chemical modified, respectively.

Table 2: Properties obtained from quantum chemical calculations at the semi empirical level for all complexes.

Complexes	Energy (eV)	ε_{HOMO} (eV)	ε_{LUMO} (eV)	E_g (eV)[a]	Dipole (D)	E_b (kcal/mol)
Δ⁹-THC-Δ⁹-THC	−7743.19	−8.50	0.24	8.74	4.80	−2.60
Δ⁹-THC-FBB	−7069.13	−13.46	−7.76	5.70	11.74	−25.37
Δ⁹-THC-TX	−11537.28	−8.62	0.32	8.94	4.58	−7.24
2Δ⁹-THC-FBB	−10941.44	−12.86	−7.52	5.34	11.13	−43.08
2Δ⁹-THC-TX	−15408.92	−8.51	0.38	8.89	4.94	−9.46
COC-CB[6]	−16659.68	−7.50	−0.09	7.41	2.84	−3.32

[a]|HOMO − LUMO|

For all conformation, from the Mayer bond order analyzes, it was not observed the formation of chemical bond between the chemical modified and drug abuse indicating the adsorption is a physical process. The Table 2 presents some electronic results obtained in these calculations.

The FBB + Nafion chemical modified was not considered because their large size and complexity to be treated using theoretical methods. The negative values of the total energy (Energy) indicate that all complexes are energetically favorable. The largest Eg for Δ⁹-THC-TX and 2Δ⁹-THC-TX complexes shows their stability in chemical reactions, contrary the Δ⁹-THC-FBB and 2Δ⁹-THC-FBB complexes are more suitable to react with others chemical species. Therefore, these results suggest that the TX can be an efficient chemical modified use in the piezoelectric system to detect Δ⁹-THC due its lowest reactivity. Moreover, the properties (Table 2) of Δ⁹-THC-Δ⁹-THC dimer are very similar with the nΔ⁹-THC-TX indicating identical interactions. The largest dipole moment for nΔ⁹-THC-FBB complexes is attributed to the charge transfers from the FBB to nΔ⁹-THC molecules. In Figure 2, the loss of mass from the piezoelectric sensor modified by the FBB is observed. A lowest Eg value (Table 2) was obtained by the nΔ⁹-THC-FBB. Therefore, the decrease of mass can be attributed to the highest interactions between the Δ⁹-THC and FBB. In this way, a possible mechanism to explain how the piezoelectric modified with FBB works was proposed. First, after the insertion of the Δ⁹-THC in the glass cell, there is a high absorption of the Δ⁹-THC by the FBB. Second, after the insertion of the N_2 gas, there is the carrying of Δ⁹-THC molecules and the some Δ⁹-THC-FBB complexes implying in the lost of mass in piezoelectric system. For the piezoelectric sensor modified by the TX, there is absorption of Δ⁹-THC mass (see Figure 3). However, Δ⁹-THC-TX and 2 Δ⁹-THC-TX complexes were observed the highest Eg (Table 2) implying in the small interactions between Δ⁹-THC and TX, but this interaction is more favorable than Δ⁹-THC-Δ⁹-THC dimer. These results indicate that the N_2 gas does not carry the Δ9-THC-TX complexes because they interactions are relatively weak. According to the Table 2, the 2Δ⁹-THC-TX complex has more 30% of interaction favorable than the Δ⁹-THC-TX dimer implying that a TX can interact with two or more Δ⁹-THC molecules efficiently than one molecule. Therefore, this result can explain the largest amount of the Δ⁹-THC drug absorbed in the piezoelectric system coated with the TX. Overall, this theoretical data was in an agreement with experimental data. Moreover, based on these semi empirical results, the piezoelectric sensor modified by the TX is more appropriated to be used to detect the Δ⁹-THC due they chemical stability.

For cucurbituril, these classes of molecules are generally used to encapsulate another chemical species. However, the calculations had shown unfavorable interactions (positive binding energy) in the encapsulation process. The COC does not bind inside the CB (6) cavity, which can be attributed to the large size of this drug abuse. On the other hands, binding energy with negative value (favorable interaction) was found when the COC were optimized at the CB (6) surface, Figure 7. In the optimized complex, the COC interact with CB (6) though the carbonyl groups at their edges see Figure 8. Therefore, our results suggest that the CB (6) chemical modified interact with the piezoelectric crystal surface using the outside of the CB (6) carbonyl groups. The stability of the complex was considered by its energy gap of 7.41 eV, which the binding energy obtained was −3.32 kcal/mol. The small frequency variation (20 Hz) observed for this system can be attributed to the weak interaction between the COC and CB (6).

Conclusion

The electrode modified with TX adsorbed the largest number of cannabinoids adsorption. However, it was not fully reversible. The electrode modified with FBB and Nafion furnished the best results: it was fully reversible for the cannabis extract. The other chemical modifiers used here could be employed in studies with cannabis extract since all the modified electrodes were reproducible in subsequent triplicate experiments. For cocaine analysis, CB (6) modifier did show good results, and this behavior and stability of the piezoelectric sensor can be useful for detection of seized samples. This study involving piezoelectric technique was considered easy to operate. The application of CB (6) modifier can be useful for detecting other drugs such as MDMA [65]. Using this technique for detecting these illicit drugs (in triplicate), a time of 12 minutes was necessary for each range of concentration.

The PM7 semi empirical method was used to understand the adsorption process of the Δ⁹-THC in the piezoelectric sensors modified. Our theoretical results show that the decrease and the increase of mass observed in the FBB and TX systems, respectively, can be explained using the binding energy between these chemical modified and Δ⁹-THC molecules.

Acknowledgement

The authors acknowledge CAPES (Edital CAPES Pro-Forenses 25/2014), and FAPESP – Fundação de Apoio a Pesquisa do Estado de São Paulo (Process 2012/00084-7 and process 2016/01447-7) for financial support.

References

1. United Nations Office on Drugs and Crime, World Drug Report 2015. Available from:http://www.unodc.org/documents/wdr2015/World_Drug_Report_2015.pdf. Accessed in December 2015.

2. E.M. Tunbridge, G. Dunn, R.M. Murray, N. Evans, R. Lister, K. Stumpenhorst, et al. Genetic moderation of the effects of cannabis: catechol-O-methyltransferase (COMT) affects the impact of Δ9-tetrahydrocannabinol (THC) on working memory performance but not on the occurrence of psychotic experiences. J Psychopharmacol. 2015; 29: 1146-1151.

3. R.M. Kaufman, B. Kraft, R. Frey R, S. Weiszenbichler, C. Bäcker, K. Kasper, et al. Acute psychotropic effects of oral cannabis extract with a defined content of Delta9-tetrahydrocannabinol (THC) in healthy volunteers. Pharmacopsychiatry. 2010; 43: 24-32.

4. L.S. Oliveira, M.A. Balbino, M.M.T. Menezes, E.R. Dockal, M.F. Oliveira. Voltammetric analysis of cocaine using platinum and glassy carbon electrodes chemically modified with Uranyl Schiff base films. Microchem. J. 2013; 110: 374-378.

5. L.S. Oliveira, A.P.S. Poles, M.A. Balbino, M.M.T. Menezes, J.F. Andrade, E.R. Dockal, et al. Voltammetric determination of cocaine in confiscated samples using a carbon paste electrode modified with differen [UO2(X-MeOsalen)(H2O)].H2O complexes. Sensors 2013; 13: 7668-7679.

6. L. Asturias-Arribas, M.A. Alonso-Lomillo, O. Domínguez-Renedo, M. J. Arcos-Martínez. Sensitive and selective cocaine electrochemical detection using disposable sensors. Anal Chim Acta. 2014; 834: 30-36.

7. M. Roushani, F. Shahdost-fard. Fabrication of an electrochemical nanoaptasensor based on AuNPs for ultrasensitive determination of cocaine in serum sample. Mater Sci Eng C. 2016; 61: 599-560.

8. A. S. Emrani, N. M. Danesh, M. Ramezani, S. M. Taghdisi, K. Abnous. A novel fluorescent aptasensor based on hairpin structure of complementary strand of aptamer and nanoparticles as a signal amplification approach for ultrasensitive detection of cocaine. Biosens Bioelectron. 2016; 79: 288-293.

9. A.R. Fukushima, V. M. Carvalho, D.G. Carvalho, E. Diaz, J.O. Bustillos, H.S. Spinosa, et al. Purity and adulterant analysis of crack seizures in Brazil. For Sci Int. 2014; 243: 95-98.

10. M.A. Balbino, I.C. Eleotério, L.S. de Oliveira, M.M.T. de Menezes, J. F de Andrade, A.J. Ipólito, et al. A comparative study between two different conventional working electrodes for detection of Δ^9-tetrahydrocannabinol using square-wave voltammetry: a new sensitive method for forensic analysis. J Braz Chem Soc. 2014; 25: 589-596.

11. Y. Tsumura, T. Mitome, S. Kimoto. False positives and false negatives with a cocaine-specific field test and modification of test protocol to reduce false decision. For Sci Int. 2005; 155: 158-164.

12. M.A. Balbino, E. N. Oiye, M. F.M. Ribeiro, J. W. Cruz Júnior, I. C. Eleotério, A. J Ipólito, et al. Use of screen-printed electrodes for quantification of cocaineand Δ^9-THC: adaptions to portable systems for forensic purposes. J Solid State Electrochem. 2016; 20: 2435-2443.

13. I.R. Nascimento, H.B. Costa, L.M. Souza, L.C. Soprani, B.B. Merloc, W.Romão. High Temperature Mass Detection Using a Carbon Nanotube Bilayer Modified Quartz Crystal Microbalance as a GC Detector, Anal Methods. 2015; 7: 1415-1424.

14. C. Fredriksson, S. Kihlman, M. Rodahl, B. Kasemo. The piezoelectric quartz crystal mass and dissipation sensor: a means of studying cell adhesion, Langmuir. 1998; 14: 248-251.

15. W.G. Cady. Piezoelectricity, 1st ed., McGraw-Hill, New York, 1946.

16. A.C. Becquerel, Bull. Soc. Philomath. 1820; 7: 149-155.

17. J. Curie, P. Curie, Bull. Soc. Min. Paris. 1880; 3: 90-93.

18. C.D. Stockbridge. Resonance Frequency versus Mass Added to Quartz Crystal. In: Vacuum Microbalance Techniques, Plenum Press, New York, 1966.

19. G. Sauerbrey. Verwendung von Schwingquarzen zur Wagung dunner Schichten und Microwagung. Z Phys. 1959; 155: 206-222.

20. G. Sauerbrey. Messung von Plattenschwingungen kleiner Amplitude durch Lichtstrommodulation. Z Phys. 1964; 178: 457-471.

21. C.C. Chen, J.S. Shih. Multi-Channel Piezoelectric Quartz Crystal Sensor with Principal Component Analysis and Back-Propagation Neural Network for Organic Pollutants from Petrochemical Plants. J Chin Chem Soc. 2008; 55: 979-993.

22. W.H. King. Piezoelectric Sorption Detector. Anal Chem. 1964; 36: 1735-1739.

23. C.W. Lee, Y.S. Fung, K.W. Fung. A piezoelectric crystal detector for water in gases. Anal Chim Acta. 1982; 135: 277-283.

24. J.P. Randin, F. Zullig. Relative humidity measurements using a coated piezoelectric quartz crystal sensor. Sens Actuators. 1987; 11: 319-328.

25. X.H.Wang, Y.F. Ding, J. Zhang, Z.Q. Zhu, S.Z. You, S.Q. Chen, et al. Humidity sensitive properties of ZnO nanotetrapods investigated by a quartz crystal microbalance. Sens Actuators B. 2006; 115: 421-427.

26. L. Chen, J. Zhang, X. H. Zhai , J. Q. Han, J. Y. Lu. Investigations of humidity properties of on indium oxide thin films coated quartz crystal microbalances. Instrumentation Science & Technology. 2012; 40: 216-225.

27. K.D. Esmeryan, T.A. Yordanov, L.G. Vergov, Z.G. Raicheva, E.I. Radeva, Humidity tolerant organic vapor detection using a superhydrophobic quartz crystal microbalance. IEEE Sens J. 2015; 15: 6318-6325.

28. D.L. Hammond, C.A. Adams, P. Schmidt, A linear. Quartz-Crystal, Temperature sensing element. Trans Instr Soc Am. 1965; 4: 349-354.

29. R.L. Chuan. An instrument for the direct measurement of particulate mass. J Aerosol Sci. 1970; 1: 111-114.

30. J.G. Olin, G.J. Sem, D.L. Christenson. Piezoelectric – Electrostatic Aerosol Mass Concentration Monitor. American Ind Hyg Assoc J. 1971; 32: 209-220.

31. P.S. Daley, D.A. Lundgren. The Performance of Piezoelectric Crystal Sensors Used to Determine Aerosol Mass Concentrations. Am Ind Hyg Assoc J. 1975; 36: 518-532.

32. R.L. Chuan. Rapid measurement of particulate size distribution in the atmosphere In: Benjamin Y.H. Liu, Editor(s), Fine Particles. Academic Press. 1976; 763-775.

33. L. Gao, Y. Yan, R. M. Carter, D. Sun, P. Lee, C. Xu. On-line particle sizing of pneumatically conveyed biomass particles using piezoelectric sensors. Fuel. 2013; 113: 810-816.

34. V.N. Morozov, I.L. Kanev, A.Y. Mikheev, E.A. Shlyapnikova, Y.M. Shlyapnikov, M.P. Nikitin, et al. Generation and delivery of nanoaerosols from biological and biologically active substances. J Aerosol Sci. 2014; 69: 48-61.

35. P. Oberg, J. Logensjo. Crystal Film Thickness Monitor, Sci. Instr. 1959; 30: 1053.

36. S.Tuukkanen,T.Julin, V.Rantanen, M.Zakrzewski, P.Moilanen, K.E. Lilja, S. Rajala. Solution-processible electrode materials for a heat-sensitive piezoelectric thin-film sensor, Synthetic Metals, Synthetic Metals. 2012; 162: 1987-1995.

37. L.J. Slutsky, W.H. Wade. Adsorpition of Gases on Quartz Single Crystals. J Chem Phys. 1962; 36: 2688-2692.

38. A. A. Duarte, L. M. G. Abegão, J. H. F. Ribeiro, J. P. Lourenço, P. A. Ribeiro, M. Raposo. Study of in situ adsorption kinetics of polyelectrolytes and liposomes using quartz crystal microbalance: Influence of experimental layout. Rev Sci Instrum. 2015; 86: 0639011-0639019.

39. R. Liang, Q.M. Wang. High sensitivity piezoelectric sensors using flexible PZT thick-film for shock tube pressure testing. Sens Actuators a Phys. 2015; 235: 317-327.

40. K. Fujii, K. Ohashi, T. Hashimoto, N. Hara, Atmospheric corrosivity estimation at electrical control unit room by multichannel quartz crystal microbalance corrosion sensors. Mater Trans. 2012; 53: 412-416.

41. G.G. Guilbault. The use of mercury (II) bromide as coating in a piezoelectric crystal detector. Anal Chim Acta. 1967; 39: 260-264.

42. A. Cavicchioli, C. A. Neves, R. I. Paiva, D. L. A. de Faria. An upgraded automatic piezoelectric quartz crystal dosimeter for environmental monitoring

in indoor cultural heritage conservation areas. Sensors and Actuators B. 2014; 190: 1014-1023.

43. W.F. Fischer, W.H. King. New method for measuring the oxidation stability of elastomers. Anal Chem. 1967; 39: 1265-1272.

44. J. Horacek, P. Skladal. Effect of organic solvents on immunoassays of environmental pollutants studied using a piezoelectric biosensor. Anal Chim Acta. 2000; 412: 37-45.

45. W. Hongmei, W. Lishi, X. Wanli, Z. Baogui, L. Chengjun, F. Jianxing. An application of artificial neural networks.Simultaneous determination of the concentration of sulfur dioxide and relative humidity with a single coated piezoelectric crystal. Anal Chem. 1997; 69: 699-702.

46. M. Benz, S. V. Patel. High temperature mass detection using a carbon nanotube bilayer modified quartz crystal microbalance as a GC detector. Anal Chem. 2015; 87: 2779-2787.

47. P. Si, J. Mortensen, A. Komolov, J. Denborg, P.J. MØller. Polymer coated quartz crystal microbalance sensors for detection of volatile organic compounds in gas mixtures. Anal Chim Acta. 2007; 597: 223-230.

48. M. Kikuch, N. Tsuru, S. Shiratori. Recognition of terpenes using molecular imprinted polymer coated quartz crystal microbalance in air phase. Sci and Tech Adv Mat. 2006; 7: 156-161.

49. S. Heydari, G.H. Haghayegh. Application of Nanoparticles in Quartz Crystal Microbalance Biosensors. Journal of Sensor Technology. 2014; 4: 81-100.

50. W.D. Hunt, D.D. Stubbs, S. Lee. I Vapor phase detection of a narcotic using surface acoustic wave immunoassay sensors. IEEE Sens J. 2005; 5: 335-339.

51. J. Halamek, A. Makover, K. Knösche, P. Skládal, F. W. Scheller. Piezoelectric affinity sensors for cocaine and cholinesterase inhibitors. Talanta. 2005; 65: 337-342.

52. J. Halamek, A. Makover, P. Skládal, F. W. Scheller. Highly sensitive detection of cocaine using a piezoelectric immunosensor. Biosens Bioelectron. 2002; 17: 1045-1050.

53. J.C. Stachowiak, M.G. von Muhlen, T.H. Li, L. Jalilian, S.H. Parekh, D.A. Fletcher. Piezoelectric control of needle-free transdermal drug delivery. J Controled Rel. 2007; 124: 88-97.

54. M.A.D. Neves, C. Blaszykowski, S. Bokhari, M. Thompson. Ultra-high frequency piezoelectric aptasensor for the label-free detection of cocaine. Biosens Bioelectron. 2015; 72: 383-392.

55. M. A. Balbino, L. S. de Oliveira, I. C. Eleoterio, E. N. Oiye, M. F.M. Ribeiro, B. R. McCord, et al. The application of voltammetric analysis of Δ9-THC for the reduction of false positive results in the analysis of suspected marijuana plant matter. J Forensic Sci. 2016; 61: 1067-1073.

56. T. Nyholm, J. P. Slotte. Comparison of Triton X-100 Penetration into Phosphatidylcholine and Sphingomyelin Mono and Bilayers, Langmuir. 2001; 17: 4724-4730.

57. W. Liu, R. Guo. Effects of Triton X-100 Nanoaggregates on Dimerization and Antioxidant Activity of Morin. Mol pharm. 2008; 5: 588-597.

58. K. R. Mahanthesha, B. E. K. Swamy, U. Chandra, T. V. Sathisha, S. Sarojini, K. V. K. Pai. Electrocatalysis of Dopamine by Alizarin and Triton-X 100 Modified Carbon Paste Electrode: A Cyclic Voltammetric Study. Anal Bioanal Electrochem. 2013; 5: 130-138.

59. B. Dong, L. Gwee, D. S. de la Cruz, K. I. Winey, Y. A. Elabd. Super proton conductive high-purity nafion nanofibers. Nano Lett. 2010; 10: 3785-3790.

60. P. Gayen, B. P. Chaplin. Selective electrochemical detection of ciprofloxacin with a porous Nafion/multiwalled carbon nanotube composite film electrode. ACS Appl Mater. Interfaces. 2016; 8: 1615-1626.

61. K. A. Page, J. W. Shin, S. A. Eastman, B. W. Rowe, S. Kim, A. Kusoglu, K. et al. In situ method for measuring the mechanical properties of Nafion thin films during hydration cycles. ACS Appl Mater Interfaces. 2015; 7: 17874-17883.

62. W. Qiu, R. Müller, E. Voroshazi, B. Conings, R. Carleer, Hans-Gerd Boyen, et al. Nafion-Modified MoO x as Effective Room-Temperature Hole Injection Layer for Stable, High-Performance Inverted Organic Solar Cells. ACS Appl. Mater Interfaces. 2015; 7: 3581-3589.

63. H. D. Correia, G. J. F. Demets. Cucurbit[6]uril/PVC-based semipermeable membranes as electrode modifiers for electrochemical investigation of insoluble substrates. Electrochem commun. 2009; 11: 1928–1931.

64. E. Blanco, C. Quintana, P. Hernández. An Electrochemical Study of Cucurbit[6]uril–Cadmium(II) Interactions and the Effect of Electrolyte Cations and Guest Molecules. Anal Lett. 2015; 48: 783-795.

65. M. C. Tadini, M. A. Balbino, I. C. Eleotério, L. S. Oliveira, L. G. Dias, G. J.F. Demets, et al. Developing electrodes chemically modified with cucurbit[6]uril to detect 3,4-methylenedioxymethamphetamine (MDMA) by voltammetry. Electrochim Acta. 2014; 121: 188-193.

66. H. Kima, J. Oha, W. S. Jeona, N. Selvapalama , I. Hwanga , Y. H. Koa, et al. A new cucurbit (6) uril-based ion-selective electrode for acetylcholine with high selectivity over choline and related quaternary ammonium ions. Supramol Chem. 2012; 24: 487-491.

67. K. I. Assaf, W. M. Nau. Cucurbiturils: from synthesis to high-affinity binding and catalysis. Chem Soc Rev. 2015; 44: 394-418.

68. K. I. Assaf, W. M. Nau. Cucurbiturils as fluorophilic receptors. Supramol Chem. 2014; 26: 657-669.

69. J.J. Stewart. Optimization of parameters for semiempirical methods VI: more modifications to the NDDO approximations and re-optimization of parameters. J Mol Model. 2013; 19: 1-32.

70. J.J.P. Stewart. Molecular Orbital PACkage. Colorado Springs, CO. 2012. Available from: http://OpenMOPAC.net (accessed 03.02.2016).

71. A. Li, H.S. Muddana, M.K. Gilson. Quantum Mechanical Calculation of Noncovalent Interactions: A Large-Scale Evaluation of PMx, DFT, and SAPT Approaches. J Chem Theory Comput. 2014; 10: 1563-1575.

72. J.G. Brandenburg, M. Hochheim, T. Bredow, S. Grimme. Low-Cost Quantum Chemical Methods for Noncovalent Interactions. J Phys Chem Lett. 2014; 5: 4275-4284.

73. B. S. De Martinis, M.F. de Oliveira. Química Forense Experimental. Cengage Learning. 2016; 512.